

Far-infrared optical properties of $\text{Bi}_2\text{Sr}_2\text{CaCu}_2\text{O}_8$

M. Reedyk, D. A. Bonn, J. D. Garrett, J. E. Greedan, C. V. Stager, and T. Timusk
Institute for Materials Research, McMaster University, Hamilton, Ontario, Canada L8S 4M1

K. Kamarás and D. B. Tanner

Department of Physics, University of Florida, Gainesville, Florida 32611

(Received 15 August 1988)

The reflectance of crystals of $\text{Bi}_2\text{Sr}_2\text{CaCu}_2\text{O}_8$ has been measured in the far-infrared region at 100 K in the normal state and at 1.5 K in the superconducting state. The normal-state properties are dominated at low frequency by a narrow Drude-like peak in the real part of the optical conductivity. At higher frequency there is substantial absorption above this Drude absorption that can be parametrized with two broad oscillators centered at roughly 400 and 1000 cm^{-1} in the optical conductivity. In the superconducting state, there is a sharp reflectance edge at 300 cm^{-1} associated with a threshold in the real part of the optical conductivity, but it is not certain that this is a conventional energy gap.

We present here recent measurements of the optical properties of crystals of $\text{Bi}_2\text{Sr}_2\text{CaCu}_2\text{O}_8$ in the far-infrared region. This member of the complicated Bi-Sr-Ca-Cu-O system has recently been shown to have a superconducting transition temperature near 85 K (Ref. 1) and thus affords an opportunity to study a new oxide superconductor with a transition temperature comparable to $\text{YBa}_2\text{Cu}_3\text{O}_{7-\delta}$. Infrared spectroscopy is a powerful tool in the exploration of the physical properties of superconductors; however, the oxide superconductors have presented several problems for the infrared spectroscopist. In principle, far-infrared measurements can be used to determine a superconductor's energy gap, 2Δ . Unfortunately, it has been shown that many of the gaplike features that appear in the reflectance of a superconducting oxide below T_c are not true energy gaps. The confusing reflectance edges often observed in $\text{La}_{1.85}\text{Sr}_{0.15}\text{CuO}_{4-\delta}$ (Refs. 2 and 3) and $\text{YBa}_2\text{Cu}_3\text{O}_{7-\delta}$ (Ref. 4) in the superconducting state are caused by zero crossings of the real part of the dielectric function rather than energy gaps. The normal-state optical properties of oxide superconductors are also controversial. The optical conductivity of all of the oxide superconductors studied to date seems to be composed of a Drude-like free-carrier peak centered at zero frequency and a broad mid-infrared absorption band centered at an energy of the order of 0.25 eV.⁵ At the present time, it is not certain whether the mid-infrared absorption band is a direct excitation or an indication that the charge carriers have an energy-dependent scattering rate.

The crystals used in the reflectance measurements were grown from a mixture of Bi_2O_3 , SrCO_3 , CaCO_3 , and CuO with a molar ratio of Bi:Sr:Ca:Cu equal to 2:2:1:3. This creates a crystal growth system where crystals with an approximate composition of $\text{Bi}_2\text{Sr}_2\text{CaCu}_2\text{O}_8$ are precipitated from a flux of CuO . The charge was loaded into a gold Bridgeman-type crucible with a 30° total angle tip. The total volume of the charge was 1.5 cm^3 . The loaded crucible was placed in a large furnace, heated to 950°C, cooled at 1.5 K/h to 750°C, cooled from 750 to 300°C at 85 K/h, and finally cooled to room temperature by turning off

the furnace. The crystal plates formed in the boule tend to grow parallel to the temperature gradient and are rarely thicker than 1 mm. The crystals cleave perpendicular to the c axis, and samples suitable for reflectance and resistivity measurements could be cleaved out of the boule. Although the surfaces used for the reflectance measurements were composed of several crystallites; all of the crystallites, were oriented with the c axis perpendicular to the sample surface. This means that the reflectance measurements presented here are probing the optical properties of the ab plane of $\text{Bi}_2\text{Sr}_2\text{CaCu}_2\text{O}_8$.

Figure 1 shows the resistivity, before and after annealing, of a piece of $\text{Bi}_2\text{Sr}_2\text{CaCu}_2\text{O}_8$ taken from the same boule as that used for the reflectance measurements. Substantial improvement in T_c and the width of the superconducting transition are obtained by annealing at 500°C. After annealing in air for 9 h and then in oxygen for 9 h (the air anneal causes most of the improvement in T_c) the

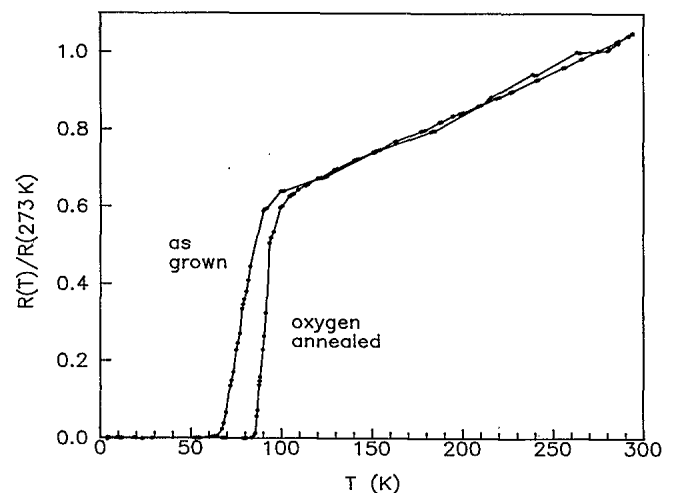


FIG. 1. dc resistivity ratio of a sample of $\text{Bi}_2\text{Sr}_2\text{CaCu}_2\text{O}_8$ before and after annealing in oxygen. Both the position and width of the superconducting transition are improved by annealing.

transition temperature was 85 K with a width (10–90%) of 8 K. Oxygen-annealed samples were used for the reflectance measurements presented below. An absolute value of the resistivity was not obtained due to the irregular shape of the samples used for resistivity measurements.

The technique used to measure the far-infrared reflectance has been described previously.⁶ The essential feature of these reflectance measurements is that *in situ* lead evaporation is used to obtain an accurate absolute value for the reflectance ($\pm 0.5\%$) despite any surface roughness. Figure 2 shows the reflectance of two $\text{Bi}_2\text{Sr}_2\text{CaCu}_2\text{O}_8$ samples both above and below T_c . The overall lower reflectance of sample B may be due to poorer quality material at the surface of the sample. The chief difficulty is that far-infrared reflectance only probes the outer micrometer or so of the sample and this thin layer of material can be disordered, oxygen depleted, off of the optimum stoichiometry, or it may contain other nonsuperconducting phases. All of these lead to surface material that is less metallic than the bulk material and this gives rise to lower reflectance. Thus, the more highly reflecting sample A gives a better measure of the absolute value of the reflectance of $\text{Bi}_2\text{Sr}_2\text{CaCu}_2\text{O}_8$. Nevertheless, there are some qualitative features that are common to both of the sets of reflectance curves presented in Fig. 2. The reflectance of both samples is very high in the normal state and there seem to be two broad reflectance edges near 300 and 500 cm^{-1} . In the superconducting state, both of these reflectance edges become considerably sharper and more pronounced and the overall far-infrared reflectance increases. Given the qualitative agreement between the two samples, it is reasonable to concentrate on the properties of the more highly reflecting sample A in the following discussion. The low-frequency reflectance of sample A in the superconducting state is slightly over 100%, although not by more than the estimated experimental uncertainty in the absolute value. In order to account for this slightly high reflectance, the data was shifted down 0.5% before being analyzed, and this adjusted

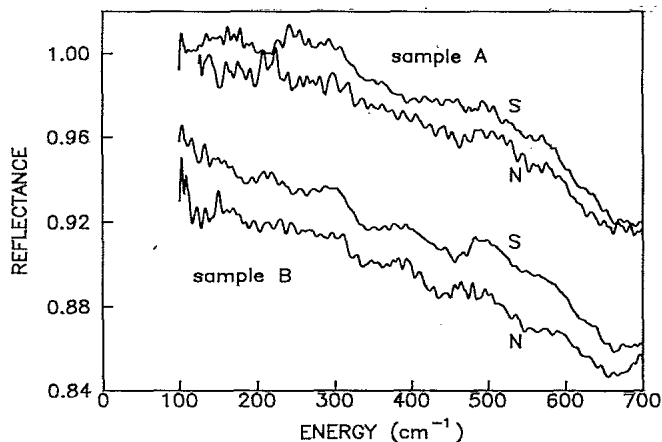


FIG. 2. Far-infrared reflectance of two samples of $\text{Bi}_2\text{Sr}_2\text{CaCu}_2\text{O}_8$ in the normal state at 100 K (N) and in the superconducting state at 1.5 K (S). Both samples exhibit reflectance edges at 300 and 500 cm^{-1} that are most clearly visible in the superconducting state.

reflectance spectrum is shown in Fig. 3.

The reflectance presented in Fig. 3 can be analyzed using Kramers-Kronig analysis and by fits of the reflectance to a Drude free-electron term and a set of harmonic oscillators.⁵ Kramers-Kronig analysis was performed using the far-infrared data at 100 K, and, at higher frequencies, recent measurements of the room-temperature reflectance up to 46000 cm^{-1} .⁷ In the normal state the extrapolation to zero frequency used in the Kramers-Kronig integral was a Drude term which fit the low-frequency-reflectance measurements.

Figure 4 shows the real part of the optical conductivity, $\sigma_1(\omega)$, obtained from Kramers-Kronig analysis of the reflectance data. The far-infrared conductivity in the normal state is dominated by a strong Drude-like peak centered at zero frequency. As was found to be the case in $\text{YBa}_2\text{Cu}_3\text{O}_{7-\delta}$,⁵ the Drude peak is followed by a very broad absorption band which causes $\sigma_1(\omega)$ to level off and then gradually rise at higher frequencies. There appears, however, to be more structure here than was observed in the $\text{YBa}_2\text{Cu}_3\text{O}_{7-\delta}$ crystals; specifically, there seems to be a broad peak in $\sigma_1(\omega)$ centered at roughly 400 cm^{-1} as well as a broad peak near 1000 cm^{-1} .

In light of the Kramers-Kronig results, the following model can be used to parametrize the optical properties of $\text{Bi}_2\text{Sr}_2\text{CaCu}_2\text{O}_8$ at 100 K in the far infrared. A Drude term is used to model the peak at zero frequency, and a set of two harmonic oscillators is used to describe the broad peak at 400 cm^{-1} and the rising conductivity at frequencies above this. A third oscillator centered at 3.5 eV is used to account for structure observed in the high-frequency reflectance.⁷ The fit of this model to the reflectance of sample A at 100 K is shown in Fig. 3. The Drude term, which is responsible for the very high reflectance at low frequency, has a plasma frequency ω_p of 11600 cm^{-1} and a scattering rate Γ of 69 cm^{-1} . The dc resistivity calculated from the Drude parameters via $4\pi\sigma_1(\omega) = \omega_p^2/\Gamma$ is 33 $\mu\Omega\text{cm}$, which is in reasonable agreement with the dc resistivity measured by Martin *et*

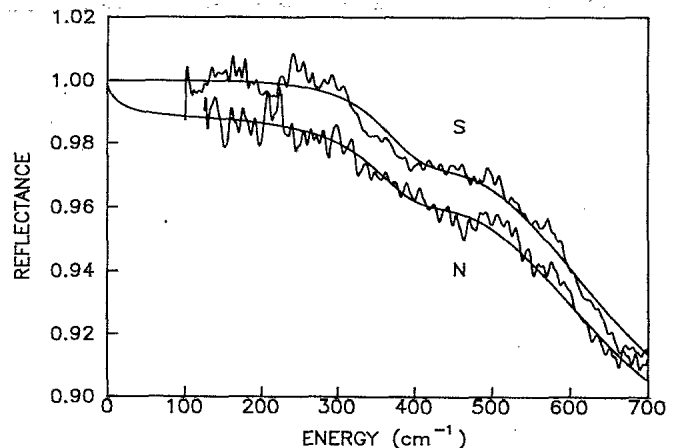


FIG. 3. The reflectance of sample A and fits of the reflectance to a Drude free-carrier term and three broad oscillators (smooth curves). The normal-state (N) curve is a least-squares fit and the superconducting-state curve (S) is generated by narrowing the normal-state Drude term to a δ function.

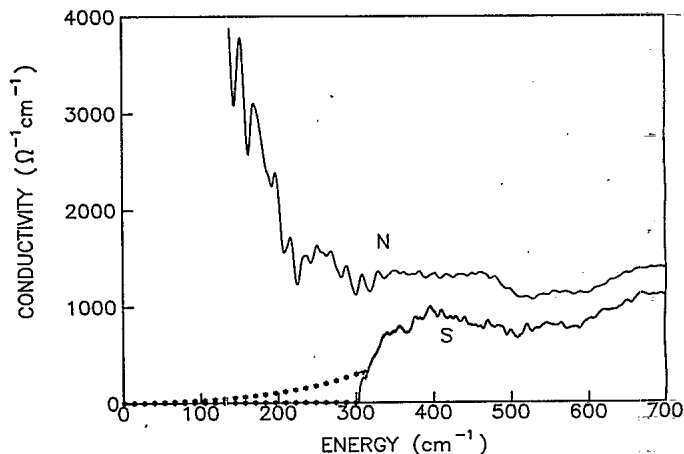


FIG. 4. The real part of the optical conductivity of $\text{Bi}_2\text{Sr}_2\text{CaCu}_2\text{O}_8$ in the normal state at 100 K (N) and in the superconducting state at 1.5 K (S) obtained by Kramers-Kronig analysis. The normal-state conductivity is dominated by a large Drude-like peak. There is also a broad peak near 400 cm^{-1} and another at higher frequency. The dotted curves show Kramers-Kronig results of two models consistent with the low-frequency reflectance at 1.5 K. The lower curve results from assuming the reflectance below 300 cm^{-1} is unity. The upper curve arises from assuming that the reflectance can be described by a δ function at the origin and a set of oscillators at higher frequency. Regardless of the extrapolation below 300 cm^{-1} , there is a sharp rise in $\sigma_1(\omega)$ above 300 cm^{-1} .

*al.*⁸ The first oscillator, which gives rise to the broad edge in the reflectance near 300 cm^{-1} , has an oscillator frequency of 412 cm^{-1} , a width of 153 cm^{-1} , and a strength of 2800 cm^{-1} . The second oscillator, which gives rise to the edge at 500 cm^{-1} in the reflectance, is centered at 996 cm^{-1} with a width of 1180 cm^{-1} and a strength of 13800 cm^{-1} .

The physical cause of the absorption above the low-frequency Drude peak in the oxide superconductors is still uncertain. There are two general classes of explanations for this absorption. First, it may simply be due to direct absorption by some strong excitation in the system:⁵ perhaps a charge-transfer excitation or two-magnon absorption. Otherwise, it might be an indication that the scattering rate of the charge carriers is energy dependent.⁹ In this view, the high-frequency $\sigma_1(\omega)$ departs from the low-frequency Drude behavior because the carriers at high frequency can be scattered by additional inelastic scattering processes. If one analyzes the $\text{Bi}_2\text{Sr}_2\text{CaCu}_2\text{O}_8$ reflectance in this way one obtains a frequency-dependent scattering rate which increases from roughly 200 cm^{-1} at low frequency to 1500 cm^{-1} at the upper limit of the far-infrared measurements. This increase in the scattering rate occurs over frequencies centered around 500 cm^{-1} , which suggests that the charge carriers are being inelastically scattered by excitations with a characteristic energy of roughly 100 cm^{-1} .

Despite the presence of two sharp edges near 300 and 500 cm^{-1} in the reflectance of $\text{Bi}_2\text{Sr}_2\text{CaCu}_2\text{O}_8$ in the superconducting state, there is no incontrovertible optical evidence of an energy gap in this material. Since there are

already broad reflectance edges at these positions in the normal state, the sharp edges in the superconducting reflectance are not necessarily energy gaps. As is suggested by measurements of the optical properties of $\text{La}_{1.85}\text{Sr}_{0.15}\text{CuO}_{4-\delta}$ (Ref. 3) and $\text{YBa}_2\text{Cu}_3\text{O}_{7-\delta}$,⁵ one may model the optical properties in the superconducting state by concentrating all of the oscillator strength of the Drude term into a δ function at the origin. Moving the Drude peak below the far-infrared region amounts to saying that, in the superconducting state, $\sigma_1(\omega)$ can be described by a δ function at origin plus the two oscillators at 400 and 1000 cm^{-1} . This approach generates the gradually rising conductivity shown, for frequencies less than 300 cm^{-1} , as a dotted curve in Fig. 4. In Fig. 3, the reflectance obtained by simply narrowing the Drude peak is shown to agree fairly well with the measured reflectance of $\text{Bi}_2\text{Sr}_2\text{CaCu}_2\text{O}_8$ in the superconducting state.

This exercise illustrates two problems in the interpretation of reflectance measurements in the superconducting state. First, it is possible to have reflectance very close to unity without the presence of an energy gap. The Drude peak narrowed to a δ function at the origin gives rise to reflectance over 0.999 at low frequencies even though the $\sigma_1(\omega)$ of this model is nonzero, as shown by the upper dotted curve in Fig. 4. A true energy gap [$\sigma_1(\omega) = 0$] in the real part of the conductivity leads to a reflectance of unity. Measurement of a reflectance of unity with an uncertainty of $\pm 0.5\%$ is not precise enough to differentiate between the perfect reflectance of an energy gap and the very high reflectance caused by the δ function at the origin in $\sigma_1(\omega)$. Second, one can have an edge in the reflectance that is not caused by sharp gap structure in the real part of the optical conductivity. The model involving a δ function at the origin and harmonic oscillators can produce the reflectance edges at 300 and 500 cm^{-1} without including a sharp absorption threshold in $\sigma_1(\omega)$. That is, the smoothly varying $\sigma_1(\omega)$ that one obtains by modeling the conductivity with a δ function and two broad oscillators can give rise to reflectance edges.

There is, however, an important difference between the measured low-temperature reflectance and the reflectance calculated from the model. The measured reflectance edge at 300 cm^{-1} is considerably sharper than the reflectance edge calculated from the oscillator model, which suggests that there may be sharp gaplike structure in $\sigma_1(\omega)$ in the superconducting state. Investigating this sharp structure by Kramers-Kronig analysis is difficult because the reflectance is so close to unity. One possible extrapolation scheme is to set the reflectance to unity up to the 300-cm^{-1} reflectance edge.⁹ As is shown in Fig. 4, the unity reflectance up to 300 cm^{-1} forces $\sigma_1(\omega)$ to be zero in that frequency range. The zero conductivity and rapid onset are consistent with a conventional superconducting energy gap at 300 cm^{-1} . However, there are other extrapolation schemes consistent with the reflectance measurements that do not force $\sigma_1(\omega)$ to be zero at low frequency. Instead of setting the reflectance to unity at low frequency, one can use the model reflectance discussed above. Using this model reflectance between 0 and 300 cm^{-1} in the Kramers-Kronig analysis gives rise to a nonzero conductivity at all frequencies, as shown in Fig. 4.

Despite the uncertainty in the low-temperature conductivity at frequencies below 300 cm^{-1} , there does seem to be an abrupt rise in the conductivity near 300 cm^{-1} regardless of the low-frequency extrapolation used. That is, the sharpness of the reflectance edge at 300 cm^{-1} in the superconducting state is due to a threshold in $\sigma_1(\omega)$ at this frequency. One cannot confidently assign this threshold to an energy gap because it is so close to the oscillator at 300 cm^{-1} . In particular, the threshold may in fact already be present in the normal state but may be obscured by the large Drude peak present above T_c .

In conclusion, far-infrared reflectance measurements in the *ab* plane of $\text{Bi}_2\text{Sr}_2\text{CaCu}_2\text{O}_8$ crystals show behavior similar to that observed in other oxide superconductors. In the normal state, the optical response is composed of a Drude-like peak centered at zero frequency followed by a broad band of absorption. Unlike $\text{YBa}_2\text{Cu}_3\text{O}_{7-\delta}$, there seems to be some structure in the mid-infrared absorption in $\text{Bi}_2\text{Sr}_2\text{CaCu}_2\text{O}_8$ since two separate oscillators are required to parametrize the shape of this absorption. It is still uncertain whether this absorption is a direct excitation or an indication that the charge carriers have an energy-dependent scattering rate. In either case, the optical measurements show that there is some excitation with

an energy of the order of tenths of an electron volt in $\text{Bi}_2\text{Sr}_2\text{CaCu}_2\text{O}_8$, and this excitation seems to be common to all of the high-temperature oxide superconductors. Two sharp reflectance edges are observed in the superconducting state, but it is not certain that either of them are associated with an energy gap. The edge at 300 cm^{-1} does seem to be associated with a sharp threshold in the conductivity, as one would expect if it were an energy gap. However, it is also possible that this feature is already present in the normal state.

We are most grateful to G. A. Thomas and J. Orenstein for discussions of the far-infrared properties of $\text{YBa}_2\text{Cu}_3\text{O}_{7-\delta}$ and to A. J. Millis, J. P. Carbotte, C. Kallin, and A. J. Berlinsky for theoretical discussions. This work was supported at McMaster University by the Natural Science and Engineering Research Council of Canada (NSERC), including infrastructure support for the Institute for Materials Research. At the University of Florida the work was supported by the National Science Foundation-Solid State Chemistry, Grant No. DMR-84-16511, and by the U.S. Defense Advanced Research Projects Agency through a grant monitored by the Office of Naval Research.

¹H. Maeda, Y. Tanaka, M. Fukutomi, and T. Asano, *Jpn. J. Appl. Phys. Lett.* **27**, L209 (1988).

²U. Walter, M. S. Sherwin, A. Stacy, P. L. Richards, and A. Zettl, *Phys. Rev. B* **35**, 5327 (1987).

³D. A. Bonn, J. E. Greedan, C. V. Stager, T. Timusk, K. Kamarás, C. D. Porter, D. B. Tanner, J. M. Tarascon, W. R. McKinnon, and L. H. Greene, *Phys. Rev. B* **35**, 8843 (1987).

⁴D. A. Bonn, J. E. Greedan, C. V. Stager, T. Timusk, M. G. Doss, S. L. Herr, K. Kamarás, and D. B. Tanner, *Phys. Rev. Lett.* **58**, 2249 (1987).

⁵T. Timusk, S. L. Herr, K. Kamarás, C. D. Porter, D. B.

Tanner, D. A. Bonn, J. D. Garrett, C. V. Stager, J. E. Greedan, and M. Reedyk, *Phys. Rev. B* **38**, 6683 (1988).

⁶D. A. Bonn, A. H. O'Reilly, J. E. Greedan, C. V. Stager, T. Timusk, K. Kamarás, and D. B. Tanner, *Phys. Rev. B* **37**, 1574 (1988).

⁷K. Kamarás (private communication).

⁸S. Martin, A. T. Fiory, R. M. Fleming, L. F. Schneemeyer, and J. V. Waszczak, *Phys. Rev. Lett.* **60**, 2194 (1988).

⁹G. A. Thomas, J. Orenstein, D. H. Rapkine, C. Capizzi, A. J. Millis, R. N. Bhatt, L. F. Schneemeyer, and J. V. Waszczak, *Phys. Rev. Lett.* **61**, 1313 (1988).